Available online at www.sciencedirect.com

SCIENCE DIRECT®

Developmental Biology 270 (2004) 364–381

DEVELOPMENTAL BIOLOGY

www.elsevier.com/locate/ydbio

Groucho homologue Grg5 interacts with the transcription factor Runx2–Cbfa1 and modulates its activity during postnatal growth in mice

WenFang Wang,[a,b] You-Gan Wang,[c] Anthony M. Reginato,[b] Donald J. Glotzer,[b] Naomi Fukai,[b] Sofiya Plotkina,[b] Gerard Karsenty,[d] and Bjorn R. Olsen[a,b,*]

[a] *Department of Oral and Developmental Biology, Harvard School of Dental Medicine, Boston, MA 02215, USA*
[b] *Department of Cell Biology, Harvard Medical School, Boston, MA 02215, USA*
[c] *Department of Statistics and Applied Probability, National University of Singapore, Singapore*
[d] *Department of Molecular and Human Genetics, Baylor College of Medicine, Houston, TX 77030, USA*

Received for publication 11 December 2003, revised 9 February 2004, accepted 4 March 2004

Available online 24 April 2004

Abstract

Runx2–Cbfa1, a Runt transcription factor, plays important roles during skeletal development. It is required for differentiation and function of osteoblasts. In its absence, chondrocyte hypertrophy is severely impaired and there is no vascularization of cartilage templates during skeletal development. These tissue-specific functions of Runx2 are likely to be dependent on its interaction with other proteins. We have therefore searched for proteins that may modulate the activity of Runx2. The yeast two-hybrid system was used to identify a *groucho* homologue, Grg5, as a Runx2-interacting protein. Grg5 enhances Runx2 activity in a cell culture-based assay and by analyses of postnatal growth in mice we demonstrate that Grg5 and Runx2 interact genetically. We also show that *Runx2* haploinsufficiency in the absence of Grg5 results in a more severe delay in ossification of cranial sutures and fontanels than occurs with *Runx2* haploinsufficiency on a wild-type background. Finally, we find shortening of the proliferative and hypertrophic zones, and expansion of the resting zone in the growth plates of $Runx2^{+/-}$ $Grg5^{-/-}$ mice that are associated with reduced *Ihh* expression and Indian hedgehog (Ihh) signaling. We therefore conclude that Grg5 enhances Runx2 activity in vivo.

Keywords: Grg5; Runx2; Yeast two-hybrid; Ihh; Growth plate; Mouse

Introduction

Runx2–Cbfa1, a DNA-binding transcription factor, plays several key roles in skeletal development (Karsenty and Wagner, 2002; Olsen et al., 2000). It is essential for the differentiation of osteoblasts, critical for chondrocyte differentiation to hypertrophy, and is important for bone matrix production by mature osteoblasts (Ducy et al., 1997; Inada et al., 1999; Kim et al., 1999; Komori et al., 1997; Otto et al., 1997). Haploinsufficiency of *Runx2* causes cleidocranial dysplasia (CCD) in mice and humans (Huang et al., 1997; Mundlos et al., 1997; Otto et al., 2002). In *Runx2* null mice, lack of osteoblastic differentiation results in the absence of bone formation, and chondrocytes in most cartilage templates fail to undergo hypertrophy, with the notable exception of distal limb cartilages. Overexpression of *Runx2* in chondrocytes promotes hypertrophy resulting in premature endochondral ossification (Takeda et al., 2001; Ueta et al., 2001). Overexpression of a dominant-negative form of *Runx2* in osteoblasts inhibits bone formation (Ducy et al., 1999), while overexpression of *Runx2* in osteoblasts also leads to bone loss (without increasing osteoclastogenesis), suggesting that Runx2 at inappropriately high levels can inhibit the process of maturation of osteoblasts to osteocytes (Geoffroy et al., 2002; Liu et al., 2001).

Runx2 is one of three Runt transcription factors in mammals (Speck et al., 1999). Runx1 is important in hematopoiesis and Runx3 may play a role as a gastrointestinal tumor suppressor and possibly a transcription factor during neurogenesis (Castilla et al., 1996; Guo et al., 2002; Inoue et al., 2002; Levanon et al., 2002; Li et al., 2002). The

* Corresponding author. Department of Cell Biology, Harvard Medical School, 240 Longwood Avenue, Boston, MA 02215. Fax: +1-617-432-0638.
E-mail address: bjorn_olsen@hms.harvard.edu (B.R. Olsen).

0012-1606/$ - see front matter © 2004 Elsevier Inc. All rights reserved.
doi:10.1016/j.ydbio.2004.03.003

Runx proteins form heterodimers with Cbfβ, a homologue of *Drosophila* Brother (Bro) and Big-Brother (Bgb) (Adya et al., 2000; Tahirov et al., 2001). The association of Cbfβ with Runx proteins facilitates their DNA binding (Tahirov et al., 2001). The phenotype of *Cbfb* null mice is similar to that of *Runx1*-deficient mice (Wang et al., 1996). Mice that express a hypomorphic allele of *Cbfb* or mice that are *Cbfb* null but are partially rescued by carrying a *Cbfb* transgene under the control of promoters expressed by hematopoietic cells exhibit a severe skeletal phenotype similar to that of *Runx2* null mice (Kundu et al., 2002; Miller et al., 2002; Yoshida et al., 2002). These findings are consistent with the in vitro evidence of heterodimerization between Cbfβ and Runx proteins and support the notion that Cbfβ plays an important role in regulating the activity of Runx2.

Runx2 is expressed in preosteoblasts, osteoblasts, prechondrocytes, and prehypertrophic chondrocytes. Its biological functions in chondrocytes and osteoblasts are clearly distinct, but the basis for this tissue specificity is unknown. At the molecular level, the tissue specificity of Runx2 function is likely to be dependent on its interaction with other transcription complex partners. In a search for additional Runx2-interacting proteins, we identified Grg5 (*groucho* related gene 5) as an interacting protein and therefore a potential co-regulator of the activity of Runx2.

Groucho-related genes (*Grg*s, also-called *TLE*s, transducer-like *Espl*) are members of a family of co-regulators that do not bind to DNA directly but modulate the activities of DNA-binding transcription factors (Chen and Courey, 2000; Stifani et al., 1992). Based on their primary structure, they can be divided into two subgroups. Members of one subgroup, Grg1–4, resemble *Drosophila Gro*, containing an N-terminal glutamine-rich (Q) domain, a glycine/proline-rich (G/P) region, a central variable region (CnC), and C-terminal WD-40 repeats. Members of this subgroup have been shown to function as transcriptional corepressors. Members of the other subgroup, including Grg5, contain only the N-terminal Q and G/P-rich domains. In contrast to Grg1–4, Grg5 is a positive modulator of Lef/Tcf transcription factors (Brantjes et al., 2001; Cavallo et al., 1998; Roose et al., 1998).

Grg5 is expressed ubiquitously in mouse tissues. Half of *Grg5* null mice exhibit a growth defect that affects the skeletal system and is associated with reduced Indian hedgehog (Ihh) signaling in the growth plates of long bones (Mallo et al., 1993, 1995; Miyasaka et al., 1993; Wang et al., 2002). Here we report that Grg5 interacts with Runx2 and acts as a positive regulator of Runx2 activity in vitro. To study the in vivo effects of this interaction, we crossbred *Runx2* heterozygous mice with *Grg5* heterozygous and null mice. Reduced Runx2 function exacerbates the body and skeletal growth defect in *Grg5* null mice. The lack of Grg5 activity aggravates defective membranous bone formation in *Runx2* heterozygous mice and causes a severe long bone growth plate defect associated with a profound reduction in Ihh signaling.

Materials and methods

Yeast two-hybrid screening

A DupLEX-A™ yeast two-hybrid kit was purchased (Origene Technologies Inc., MD) and used in this study.

Bait construction

We constructed a LexA-Runx2 bait based on previously published data and two initial observations during this study. First, we made a LexA-Runx2 construct. A pair of primers, 5′ CCG GGA TCC ATC CGA GCA CCA GCC GGC GCT TC 3′ and 5′ CCG CTC GAG TCA ATA TGG CCG CCA AAC AGA CTC 3′, was used to amplify Runx2 cDNA from a pool of mouse E13.5 embryonic cDNAs reversely transcribed from total RNA. This cDNA, flanked by *Bam*H1 and *Xho*I restriction enzyme sites, covered the entire coding region of *Runx2*, from the N-terminal sequence DPSTSRRF to the carboxyl end. The cDNA was inserted into pBluescript vector and then moved to the bait vector pEG202 resulting in an in-frame fusion of Runx2 with LexA DNA binding protein. In initial experiments, we observed that transformants containing the constructed plasmid grew poorly on the selective media. The mechanism of toxicity was unclear and was not studied further. Second, we made the chance observation that the toxicity of the bait could be alleviated by mutations in the Runt domain. Two nucleotide substitutions, accidentally generated by PCR, caused two amino acid changes in the Runt domain; a lysyl residue was replaced by arginine and a threonyl residue was replaced by isoleucine. No mutations were found in other regions of this PCR product. A bait containing Runx2 with these two mutations in the Runt domain was no longer toxic, but unfortunately autoactivated the reporter *Lac*Z. To overcome this autoactivation, we expanded an 18-residue alanyl stretch in the N-terminal portion of Runx2 to 27 alanyl residues. An alanyl expansion in Runx2 can cause cleidocranial dysplasia, suggesting loss of Runx2 activity in humans (Mundlos et al., 1997; Thirunavukkarasu et al., 1998). In addition, the presence of 27 alanyl residues in murine Runx2 abolishes transcriptional activity in luciferase reporter assays (Thirunavukkarasu et al., 1998). Therefore, the DNA fragment encoding the18 alanyl residues in Runx2 was replaced with a DNA segment encoding an expanded 27 alanyl residues. The final bait used in the screening, LexA-Runx2mut27, contained a 27-residue expanded alanyl stretch at the N-terminal part of Runx2 and the above two base substitutions in the Runt domain. The LexA-Runx2mut27 bait was utilized to search for Runx2-interacting proteins using an embryonic cDNA E13.5 library.

E13.5 cDNA library

Total RNAs were extracted from E13.5 embryos by the guanidine thiocyanate method followed by ultracentrifugation (Sambrook et al., 1989). Polyadenylated RNA was purified from total RNAs using an oligodT column (Prom-

ega, WI). The cDNAs were synthesized with a cDNA synthesis kit (Stratagene, CA), ligated to *Eco*RI adaptors, and inserted into pJG4–5 plasmid containing the transcription activation domain B42. The ligation mixture was desalted and electroporated into *Escherichia coli* strain XL-1Blue. A cDNA library of 2.0×10^6 independent transformants was obtained.

Construction and screening of yeast library

Both LexA-Runx2mut27 bait plasmid and a reporter plasmid pSH18–34 (*Lac*Z reporter) were transformed into yeast host EGY48 (bait host). The cDNA plasmid library was used to transform the bait host. About 5×10^5 yeast transformants were obtained and were used for the screening for Runx2-interacting proteins.

The yeast cells, containing the bait plasmid, the *Lac*Z reporter plasmid, and the cDNA library plasmids, were incubated in galactose-containing selective media for 2 h and then plated on galactose and X-gal media in the absence of leucine supplement. The blue colonies that grew on those media were streak-purified and tested again for growth in the absence of leucine supplement and for β-galactosidase (*Lac*Z) activity. Plasmids from positive colonies were extracted and transformed into the Trp^- *E. coli* strain KC-8 to recover Trp^+ prey cDNA plasmid. The recovered plasmid cDNAs were sequenced using primers flanking the insert. Homology searches were performed to identify the cDNA sequences.

Cell culture, Runx2 activity assay, and co-immunoprecipitation

COS-7 cells were maintained in DME high glucose media supplemented with 10% FBS (Irvine Scientific, CA). The transcriptional activity of Runx2 was assayed as luciferase units using the 6OSE2-luc reporter. Cells were seeded at a density of $2 \times 10^4/cm^2$ grown overnight before transfection so that confluency reached about 90%. Three plasmids, each with the CMV promoter controlling the transcription of β-galactosidase (to normalize the luciferase units), *Grg*s, or *Runx2*, were co-transfected with a luciferase reporter plasmid 6OSE2-Luc into COS-7 cells using transfection reagent GenePorter (Genome Therapeutic System, CA) according to the manufacturer's protocol. For the detection of protein levels, Runx2 and Grgs were tagged at N-terminus with HA- and FLAG-epitopes, respectively. Expression levels of the proteins in transfected cells were examined by Western blotting using anti-HA antibodies for Runx2 constructs (Santa Cruz, CA) and anti-FLAG antibodies for Grg constructs (Sigma, MO). With the exception of the ΔN1–94 and ΔQA48–94 Runx2 constructs, no significant differences in levels of expression were seen among the different Runx2-truncated proteins (Fig. 2B) and different Grgs (data not shown). As controls for transfection, we replaced *Grg*s or *Runx2* plasmids with the corresponding vectors only. Thirty-six hours later, the transfected cells were lysed with lysis buffer (Promega, WI) after two PBS washes. The total cell extract was centrifuged to remove cell debris and the supernatant was collected. Luciferase activity was assayed with the substrate kit and measured with Monolight Luminometer 2010 (Analytical Luminescence Laboratory, San Diego, CA). For immunoprecipitation, FLAG-tagged Grg5ΔN27 and HA-tagged Runx2 constructs were transiently co-transfected into COS-7 cells. Cells were lysed in LIPA buffer (25 mM Tris–HCl pH 7.5, 150 mM NaCl, 2 mM EDTA pH 8.0, 0.5% NP-40) with protease inhibitor cocktails (Sigma). Supernatants of cell lysates were incubated with anti-FLAG agarose beads (Sigma) at 4°C overnight. The agarose beads were washed with LIPA buffer three times before boiled in loading buffer for Western blots.

Mice

Heterozygous *Runx2* and *Grg5* mice were obtained from the laboratories of Dr. M. Owen and Dr. T. Gridley, respectively. The *Runx2* mice were first crossed with C57Bl/6 and the heterozygotes were then mated with *Grg5* heterozygotes or homozygotes. The compound mice $Runx2^{+/-}$ $Grg5^{-/-}$ were obtained from matings between $Runx2^{+/+}$ $Grg5^{+/-}$ and $Runx2^{+/-}$ $Grg5^{+/-}$ or $Runx2^{+/-}$ $Grg5^{+/-}$ and $Runx2^{+/+}$ $Grg5^{-/-}$. Both sexes of $Runx2^{+/-}$ $Grg5^{-/-}$ were infertile, a defect in reproduction not studied further. The mice were housed as described (Wang et al., 2002).

Growth curves

Growth curves in this study were derived as described (Wang et al., 2002). Briefly, mice were identified by an ear numbering system at about 2 weeks of age. Whole body weight was measured at least twice per week. Preliminary plots showed that the weight increase of mice was linear with age up to 20 days after birth and also linear between days 20 and 40, but growth rates clearly differed between these two periods. After day 40, the growth rate appeared to be close to zero and the body weight approached maximum. Both the growth rates and the asymptote for weight showed great variability between different mice. To allow individual variability to be incorporated into the analysis, we assumed growth parameters to be random and used the nonlinear mixed-effects model (NLME model) for calculations (Pinheiro and Bates, 2000). The following logistic model was fitted for each gender separately:

$$\text{Weight} = A/(1 + \exp^{(B-\text{days})/C})$$

The parameter A is the asymptotic (maximal) weight for each individual mouse, B is the age (in days after birth) when the weight reaches half of the maximum, C is a measure of relative growth rate, that is, how fast the weight approaches the maximal weight and is the difference of the numbers of days when the weight is $1 / (1 + e^{-1})$ of its maximum and the weight is half of its maximum. The growth rate (calculated

by taking the derivative with respect to age) can be written as $p\ (1 - p)\ A\ /\ C$, where p = weight/A is the proportion of weight to the maximal weight. The NLME model in S^+ (version 5) was used to obtain the parameter estimates.

Values for A, B, and C were assumed to vary for different genotypes. The parameter A was assumed to be random to account for individual variability and litter effects on growth, that is, the mother and father of individual mice were assumed to contribute in a random fashion ($\ln A$ normally distributed). Both parameters B and C were assumed to be fixed to avoid spurious results because of high intrinsic correlation.

Skeletal staining

Three-week-old mice were CO_2 euthanized, deskinned, and eviscerated. The skeletons were then immersed for 10 days in a staining solution containing alizarin red, alcian blue, ethanol, and acetic acid. The stained skeletons were clarified with 1.8% KOH overnight followed by 1 week in 0.3% KOH. The stained skeletons were stored in 100% glycerol.

Histology

Histological studies were carried out as described (Wang et al., 2002). Briefly, the tibiae and humeri were dissected and fixed in 4% paraformaldehyde (PFA) in PBS for 1 week at 4°C. Decalcification took place in 0.5 M EDTA pH 7.4 (pH adjusted with citric acid powder) with a change of solution every day. The tissues were dehydrated in an ascending ethanol series, infiltrated with paraffin through xylene, and embedded in the desired orientation. Samples were cut into longitudinal 5-μm sections with a HM355 Microtome, mounted onto Superfrost Plus slides (VWR), and dried on a heated plate at 45°C overnight. The sections were stained with hematoxylin and eosin using a standard protocol.

Immunohistology

Bone sections for immunostaining were deparaffinized in xylene and rehydrated in a descending ethanol series before being processed for immunostaining in a Biogenex automated processor. Antibodies against proliferating cellular nuclear antigen (PCNA), Indian hedgehog (Ihh), Smoothened (Smo), Patched (Ptc), and parathyroid hormone-related peptide (PTHrP) were purchased from Research Antibodies (Santa Cruz, CA). A mouse monoclonal antibody against collagen type II was purchased from LabVision (San Diego, CA) and used in conjunction with the MOM kit (Vector Laboratory, CA) to decrease background staining. To compare Ihh expression at the protein level in growth plates, equivalent areas in each Ihh-immunostained section were selected for counting of Ihh-positive cells. The Ihh-positive cell numbers from two sections from each individual mouse, with three mice used for each genotype, were averaged and expressed as a percentage of the number of Ihh-positive cells in sections of *Runx2*$^{+/+}$ *Grg5*$^{+/-}$ mice (set at 100%).

In situ hybridization

Radioactive in situ hybridization with ^{33}P-labelled probes on tissue sections was performed as described (Hartmann and Tabin, 2000). The probes for *Col1a1*, *Col2a1*, *Col10a1*, and *Ihh* were the gifts of E.J. Reichenberger, N. Fukai, S. Apte, and A. McMahon, respectively.

Results

Grg5 interacts with Runx2

A yeast two-hybrid system was used to search for Runx2-interacting proteins. We used LexA-Runx2mut27 as the bait and a mouse E13.5 cDNA plasmid library as the prey (see Materials and methods). Approximately 5×10^5 independent yeast transformants were screened resulting in the isolation of over 500 candidate clones. Sequence analysis revealed that one of these clones was isolated four times and represented a truncated version of Grg5 (Fig. 1A). The fused target B42-Grg5ΔN27 contained most of the Grg5 amino acid sequence but lacked the first 27 amino acid residues at the N-terminus (GenBank accession number L12140). The interaction between LexA-Runx2mut27 and B42-Grg5ΔN27 was confirmed by transforming the corresponding plasmids back into yeast cells with LexA-Runx2mut27, the *Lac*Z reporter plasmid, and B42-Grg5ΔN27 (Fig. 1B). To exclude a possible effect of the lack of the very N-terminal 27 amino acid residues of Grg5ΔN27 on the interaction with Runx2, full-length *Grg5* was amplified by PCR and also fused to B42. No difference was found between the truncated Grg5ΔN27 and full-length Grg5 when their plasmids were compared in yeast cells with "full-length" Runx2 (LexA-Runx2mut27, data not shown). Therefore, the first 27 amino acid residues at the N-terminus of Grg5 are not required for the interaction between Runx2 and Grg5 in yeast.

To examine the Grg5-interacting region in Runx2, a series of LexA-Runx2mut27 deletion constructs was made and tested for interactions with Grg5ΔN27 (Fig. 1B). The results showed that the C-terminal portion of Runx2 was sufficient for activation of the *Lac*Z reporter and growth in the absence of leucine. Moreover, the removal of the C-terminal sequence VWRPY had no effect on the interaction between Runx2 and Grg5ΔN27, a finding that contrasts with the importance of this C-terminal sequence for the interaction between Runt and Gro in *Drosophila* (Aronson et al., 1997). In summary, the Grg5-interacting domain of the Runx2 protein resides within the C-terminal 141 amino acid residues but does not require the last 5 amino acid residues.

Grg3b, a short form of Grg3, shares a similar primary protein structure with Grg5 (Fig. 1C; Leon and Lobe, 1997; Yao et al., 1998). Because both Grg3b and Grg5 are members of the subfamily of short Grg proteins, homologous to the N-terminal region of the long Grg family members, we compared their interaction with Runx2. Although yeast cells

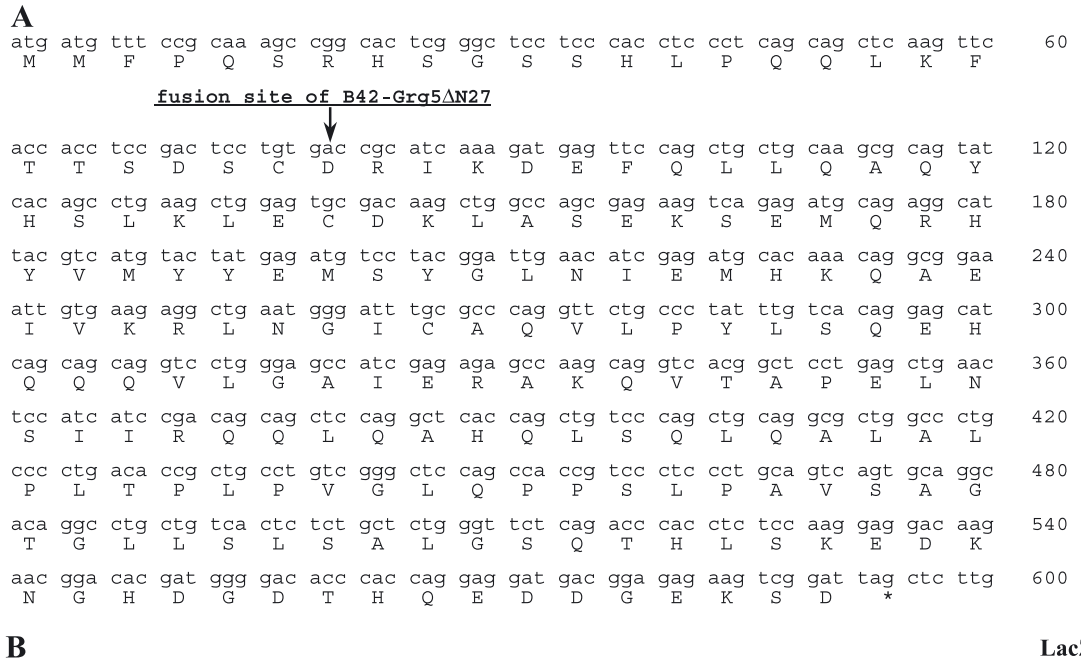

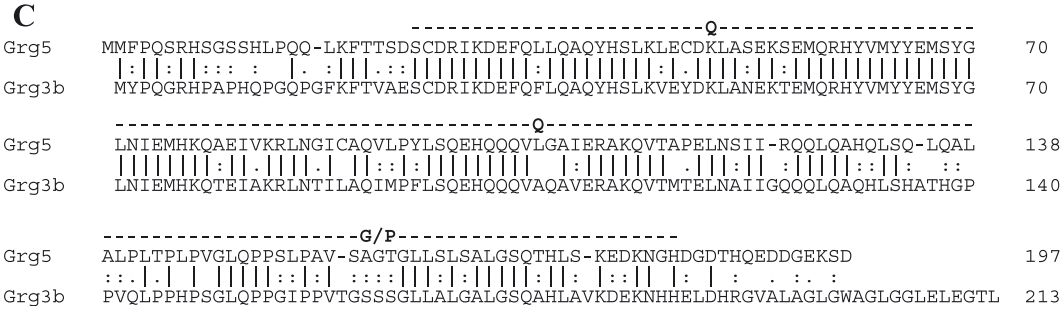

containing Grg3b grew poorly on a galactose-containing medium, the same region in Runx2 was clearly involved in the interactions between Runx2 and Grg5 or Grg3b (Fig. 1B). Because Grg3b and Grg5 share 73% amino acid identity in the middle Q- and GP-rich regions while the N- and C-terminal regions are completely different (Fig. 1C), we conclude that the middle portion (Q and GP domains) of Grg5 is most likely responsible for the interaction with Runx2.

Grg5 enhances whereas Grg3 inhibits Runx2 activity

To determine the effect of the Grg5 interaction with Runx2, we first measured Runx2 transcriptional activity in the absence or presence of Grg5ΔN27 using the 6OSE2-Luc reporter (Fig. 2). When wild-type *Runx2* was co-transfected with Grg5ΔN27 into COS-7 cells, the reporter luciferase activity was increased at least 3-fold. We further constructed a series of Runx2 deletions to test how the Grg5-interacting domain in Runx2 affects the transcriptional activity (Fig. 2). Consistent with the yeast two-hybrid data, the increased activity of Grg5ΔN27 was correlated with the presence of the Grg5-interacting domain in Runx2. Without the Grg5 binding domain, no enhancement of Runx2 activity by Grg5ΔN27 was seen. Similar to the yeast two-hybrid assay, we also assayed the ability of full-length Grg5 to coactivate Runx2. The full-length Grg5 acted like Grg5ΔN27 on Runx2 activation as expected except in the case of three Runx2 deletion constructs, ΔN1–48, ΔN1–94, and ΔC516–528, encoding Runx2 proteins that lack the N- or C-terminal regions. This suggests that the N-terminal 27 amino acid residues of Grg5 may exert an inhibitory effect on Grg5 coactivation in the absence of the N- or C-terminal regions of Runx2 (see Discussion). In contrast to Grg5 and Grg5ΔN27, Grg3 repressed Runx2 transcriptional activity to background levels (Fig. 2). However, unlike full-length Grg3, Grg3b appeared to lack specificity in transcriptional repression because it not only repressed the Runx2 reporter but also reduced the activity of an internal control, β-galactosidase (data not shown).

We also performed similar transfection assays in three other cell lines, ROS17/2.8 (rat osteosarcoma cell line), MC3T3-E1 (mouse osteoblastic cell line), and ADTC5 (mouse chondrogenic cell line). The results with MC3T3-E1 cells were similar to those with COS-7 cells despite a low transfection efficiency (data not shown). A less striking increase in Runx2 activity (30–50%) was observed with both ADTC5 and ROS17/2.8 cells in the presence of Grg5. In the case of ROS17/2.8 cells, the low enhancement could be due to a high level of endogenous Grg repressor proteins in this cell line (Levanon et al., 1998; Thirunavukkarasu et al., 1998).

To provide biochemical evidence for a Grg5–Runx2 interaction in COS-7 cells, we used FLAG-tagged Grg5ΔN27 to pull down HA-tagged Runx2 proteins in COS-7 extracts. As expected, full-length Runx2, ΔN1–48, and ΔC516–526 proteins were detected in protein complexes pulled down with anti-FLAG agarose beads whereas ΔC375–528, ΔC275–528, and control vectors were not (Fig. 2B and see the legend). The co-immunoprecipitation results support the conclusion, based on the yeast two-hybrid assays, that there is a physical interaction between Grg5 and Runx2.

In vivo effects of Grg5 and Runx2 interaction

To study the in vivo effects of Grg5 and Runx2 interactions, we crossbred mice with gene-targeted *Runx2* and *Grg5* alleles. We have previously shown that *Grg5* null mice have a skeletal growth defect associated with reduced Ihh signaling in the growth plates (Wang et al., 2002). If Runx2 is a major target of Grg5, we hypothesized that osteoblasts and chondrocytes would display reduced Runx2 function in the absence of Grg5, especially in the $Runx2^{+/-}$ $Grg5^{-/-}$ mouse. To generate these mice, we crossed $Runx2^{+/-}$ $Grg5^{+/-}$ animals with heterozygous $Grg5^{+/-}$ or homozygous $Grg5^{-/-}$ mice. Similar to the experience with *Grg5* null mice (Mallo et al., 1995; Wang et al., 2002), no abnormal embryonic or postnatal lethality was observed in $Runx2^{+/-}$ $Grg5^{-/-}$ mice. The percentage of $Runx2^{+/-}$ $Grg5^{-/-}$ mice was close to the expected numbers. The observed numbers from the crosses between $Runx2^{+/+}$ $Grg5^{+/-}$ females and $Runx2^{+/-}$ $Grg5^{+/-}$ males were 87:200:94:70:170:60 (Mendelian ratio 1:2:1:1:2:1) for the different genotypes (Runx2 Grg5) +/+ +/+, +/+ +/–, +/+ –/–, +/– +/+, +/– +/–, +/– –/–.

To study the overall growth of $Runx2^{+/-}$ $Grg5^{-/-}$ mice, we used a nonlinear statistical model as previously described for *Grg5* null mice (Wang et al., 2002) to derive the growth curves for the six possible genotypes. We compared

Fig. 1. Grg5 and its interaction with Runx2. (A) *Grg5* nucleotide (top) and the derived amino acid (bottom) sequences based on GenBank accession number L12140. The vertical arrow between nucleotides 80 and 81 (nucleotide numbers at the right) indicates the site at which the *Grg5* cDNA was fused in frame to the upstream B42, using an adaptor oligonucleotide, 5′ GAA TTC GGC ACG AG 3′, to join the B42 sequence to the *Grg5DN27* sequence. (B) Both Grg5 and Grg3b interact with the C-terminal portion of Runx2. Diagrams of a series of LexA-Runx2 bait constructs are shown at the left. The Runx2 portion of the full-length bait (top) contains an N-terminal activation domain, a glutamine and alanine-stretch (QA27) (in which the normal polyalanine sequence has been expanded to 27), the Runt domain, a nuclear localization sequence (NLS), and a PST-rich domain. The two mutations in the LexA-Runx2mut27 bait are indicated with two asterisks. Deletion constructs were made and given designations (at left) that reflect either the deleted regions or the remaining protein segments of Runx2. The C-terminal VWRPY sequence is shown at the end of the full-length bait. For each bait, four yeast transformants were used to test for β-galactosidase activity (blue patches) with either B42-Grg5ΔN27 or B42-Grg3b as preys (results shown at right). (C) Alignment of Grg5 (top) and Grg3b (bottom) protein sequences. Amino acid residue numbers at right. The amino acid identity between Grg5 and Grg3b is high in the Q- and G/P- domains (dashed line above the sequences) and low at N- and C-terminal regions.

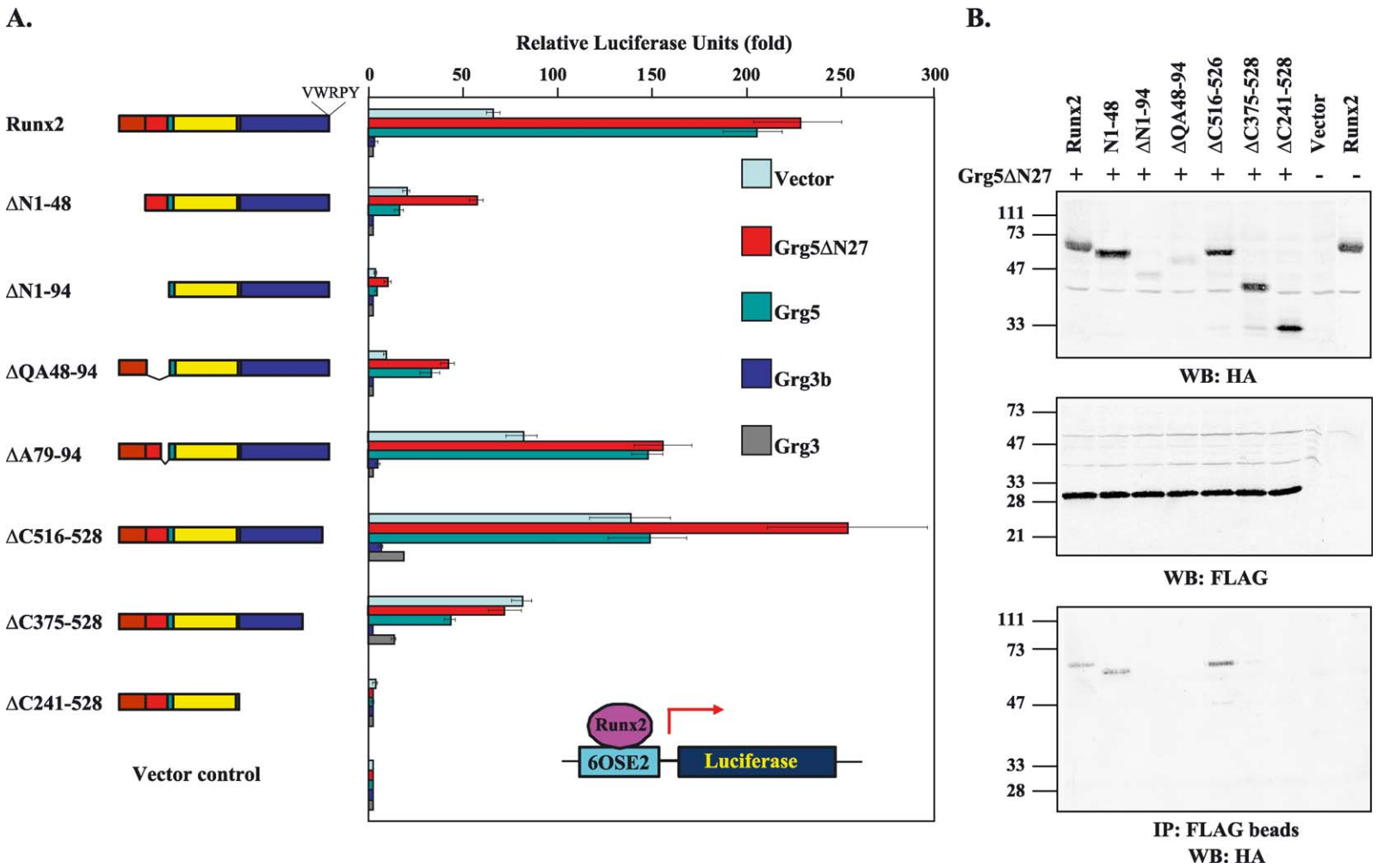

Fig. 2. Functional and structural interactions between Grg5 and Runx2 proteins in COS-7 cells. (A) Runx2 activity was assayed in COS-7 cells with 6OSE2-Luc reporter (diagram within bar graph at bottom) by transient transfection. Different *Runx2* constructs (diagrams at left) were co-transfected with *Grg*s or vector alone (colored-coded and shown within bar graph at top right). All constructs were driven by the CMV promoter and tagged with either HA- or FLAG- epitopes (see Materials and methods). The domain structure of full-length Runx2 protein is as described in Fig. 1B. The deleted regions of Runx2 proteins in the constructs are indicated at left; the amino acid residues are numbered according to the type II Runx2 protein sequence (GenBank accession number NM_009820). Bar graph shows luciferase units normalized to a β-gal internal control. Three separate readings from three transfections were combined and averaged. Error bars are placed on each bar. Note, the lack of enhancement with the constructs ΔN1–48, ΔN1–94, and ΔC516–528 in the presence of full-length Grg5 in comparison with Grg5ΔN27 (see Results and Discussion). (B) Co-immunoprecipitation of FLAG-tagged Grg5ΔN27 and Runx2 proteins in extracts of COS-7 cells. Top and middle panels show detection of HA-tagged Runx2 proteins (WB/HA) and FLAG-tagged Grg5ΔN27 (WB/FLAG) in Western blots of extracts. Bottom panel shows detection by Western blot of Runx2 proteins in co-immunoprecipitates obtained with anti-FLAG-conjugated agarose beads. About 90% of FLAG-tagged Grg5ΔN27 was bound to anti-FLAG agarose, whereas only about 1% of Runx2 protein came down with the agarose. Molecular weight markers are shown on left. The minor band under the 47-kDa marker across all the lanes in the top panel is a nonspecific band resulting from the use of an HA polyclonal antibody; the low level of expression of ΔN1–94 and ΔQA48–94 Runx2 deletion constructs resulted in no detectable bands in the co-immunoprecipitation assay.

the growth of 101 of the *Runx2*$^{+/-}$ *Grg5*$^{-/-}$ mice with their littermates by measuring body weights during the first 10 weeks after birth (Fig. 3). The growth curves of wild-type and *Runx2*$^{+/+}$ *Grg5*$^{+/-}$ mice overlapped. Weight gain and rate of growth in *Grg5* null, *Runx2*$^{+/-}$ *Grg5*$^{+/-}$, and *Runx2*$^{+/-}$ *Grg5*$^{-/-}$ mice were significantly lower than in wild-type animals before 4 weeks of postnatal growth ($P < 0.001$; Fig. 3). Consistent with the growth curves of *Grg5* null mice from *Grg5* heterozygous matings, we obtained similar growth curves for *Grg5* null mice (*Runx2*$^{+/+}$) in this study (Fig. 3). This growth defect was most severe in the *Runx2*$^{+/-}$ *Grg5*$^{-/-}$ mice, as shown also in skeletal preparations and whole body radiographs (Figs. 4A and B). A phenotype of dwarfism and osteopenia was apparent 1 week after birth and became severe at 2–4 weeks after birth. Most of the affected *Runx2*$^{+/-}$ *Grg5*$^{-/-}$ mice recovered to some degree after 5 weeks of age, but nevertheless the mice remained smaller than their littermates.

Similar to the findings for *Grg5* null mice (Wang et al., 2002), the severity of the growth defect in *Runx2*$^{+/-}$ *Grg5*$^{-/-}$ mice varied among individuals. Despite the individual variation, we could clearly identify the effect of the lack of *Grg5* on the phenotype associated with one copy of *Runx2*. Half of *Grg5* null mice (*Runx2*$^{+/+}$) exhibit a growth defect (Wang et al., 2002) with body weights ranging from 50% to 75% of wild-type or heterozygous *Grg5* mice and this was confirmed in this study. Only minor weight differences were seen between wild-type and *Runx2*$^{+/-}$ *Grg5*$^{+/+}$ mice (Fig. 3), but most of the *Runx2*$^{+/-}$ *Grg5*$^{-/-}$ mice (80%) had body weights in the range of 28–75% of the control wild-type or *Runx2*$^{+/+}$ *Grg5*$^{+/-}$ littermates. The weights of about 20% (21/101) of *Runx2*$^{+/-}$ *Grg5*$^{-/-}$ mice were below half the weight of wild-type littermates while about 30% (30/101) were between 50% and 60%. These numbers strongly suggest that having only one copy of Runx2 in mice exacerbates the growth defect in affected

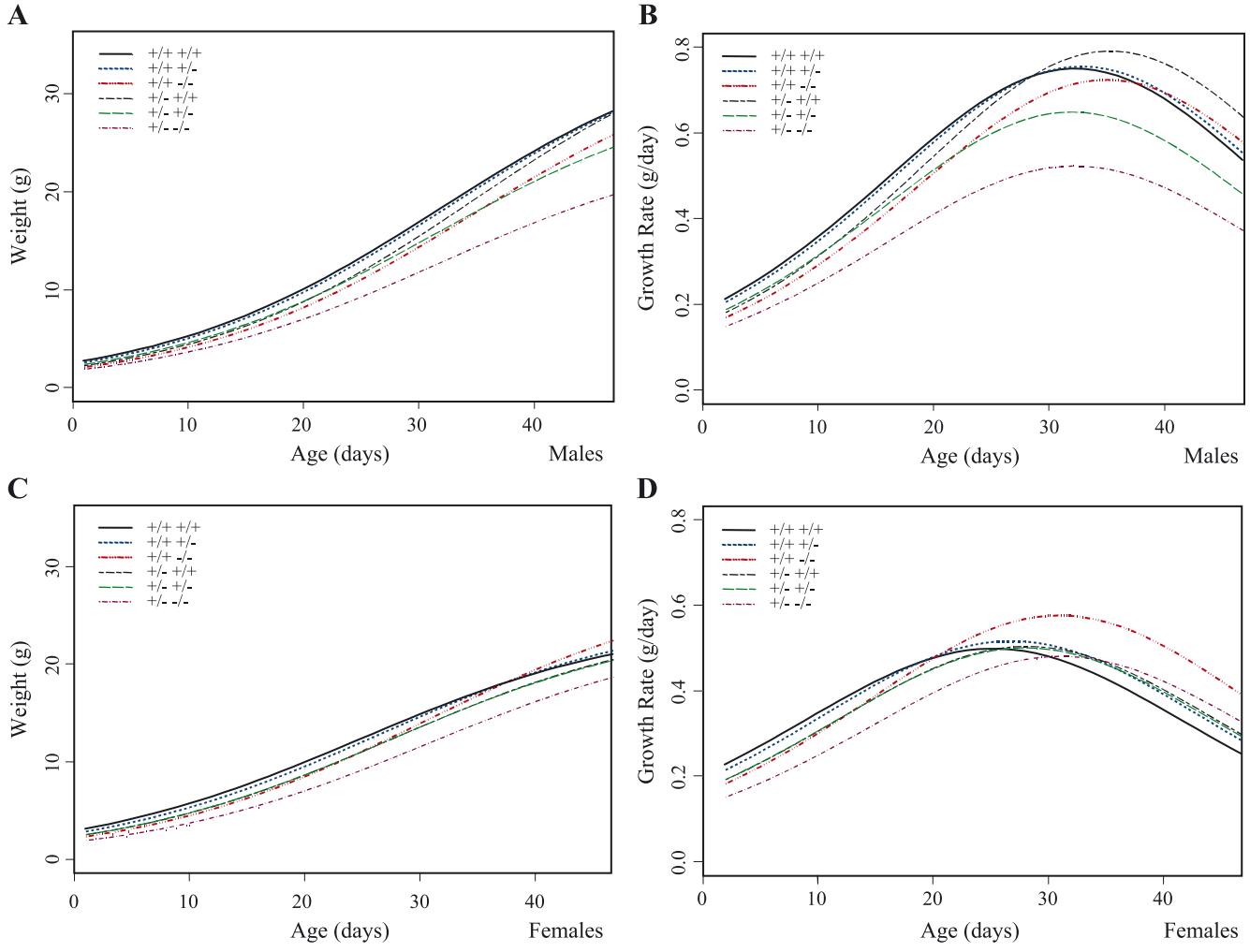

Fig. 3. Growth curves of mice with *Runx2*$^{+/+}$ *Grg5*$^{+/+}$, *Runx2*$^{+/+}$ *Grg5*$^{+/-}$, *Runx2*$^{+/+}$ *Grg5*$^{-/-}$, *Runx2*$^{+/-}$ *Grg5*$^{+/+}$, *Runx2*$^{+/-}$ *Grg5*$^{+/-}$, and *Runx2*$^{+/-}$ *Grg5*$^{-/-}$. The weights of mice were measured and the weight data were fitted in a statistical model (see Materials and methods). (A and C) Weight (expressed as Weight = $A/(1+\exp^{(B\text{-days})/C})$) vs. age for males and females. (B and D) Growth rate vs. age for males and females. The curves for mice with genotypes *Runx2*$^{+/+}$ *Grg5*$^{+/+}$ and *Runx2*$^{+/+}$ *Grg5*$^{+-}$ are essentially identical. The values for parameter *B* (see Materials and methods) of mice with genotypes of *Runx2*$^{+/+}$ *Grg5*$^{-/-}$, *Runx2*$^{+/-}$ *Grg5*$^{+/+}$, *Runx2*$^{+/-}$ *Grg5*$^{+/-}$, and *Runx2*$^{+/-}$ *Grg5*$^{-/-}$ are all significantly different ($P < 0.001$) from wild-type mice.

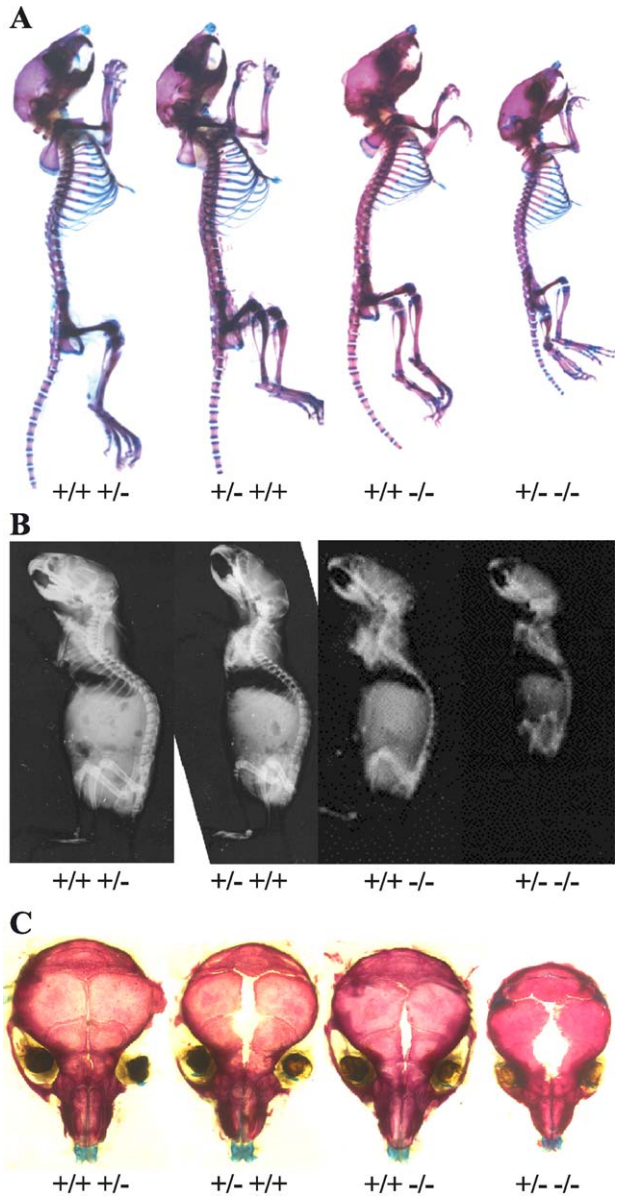

Fig. 4. Skeletal phenotypes of 3-week-old *Runx2*$^{+/-}$ *Grg5*$^{-/-}$ mice. (A) Skeletal staining of littermate mice of four different genotypes, *Runx2*$^{+/+}$ *Grg*$^{+/-}$, *Runx2*$^{+/-}$ *Grg5*$^{+/+}$, *Runx2*$^{+/+}$ *Grg5*$^{-/-}$, and *Runx2*$^{+/-}$ *Grg5*$^{-/-}$. Note the proportionately smaller skeleton in *Runx2*$^{+/-}$ *Grg5*$^{-/-}$ mouse. (B) Lateral radiographs of mice with the above genotypes. Low bone density is seen in the radiograph of *Runx2*$^{+/-}$ *Grg5*$^{-/-}$ mouse. (C) Top view of cranial bones in mice shown in A. Note that although the separation between the parietal and frontal bones in *Runx2* heterozygous mouse is an artifact generated during skeletal staining, the anterior fontanel is moderately enlarged. The lack of ossification in the anterior fontanel region and along the sagittal suture is most severe in the *Runx2*$^{+/-}$ *Grg5*$^{-/-}$ mouse. The slit-like opening seen in the *Runx2*$^{+/+}$ *Grg5*$^{-/-}$ mouse is an artifact because it was not a consistent feature of Grg5 null mice.

Grg5 null mice. No significant sex differences were seen during the first 5 weeks of postnatal growth, but later the weight differences between the female *Runx2*$^{+/-}$ *Grg5*$^{-/-}$ and wild-type mice were not as large as they were in males (Fig. 3).

The growth rates for male *Runx2*$^{+/-}$ *Grg5*$^{-/-}$ mice were the lowest of all mice studied (Figs. 3A and B). The weight gap between the male *Runx2*$^{+/-}$ *Grg5*$^{-/-}$ mutant and wild-type mice became larger with age and the mutant mice remained smaller up to 6 months of age. This deleterious effect of loss of Grg5 on Runx2 function continued to be observed after 5 weeks of age in males when the growth rate of *Runx2*$^{+/-}$ *Grg5*$^{+/+}$ mice had caught up with wild-type animals (Fig. 3B). For females, the weight difference between wild-type controls and *Runx2*$^{+/-}$ *Grg5*$^{-/-}$ mice was less than that for the males (Figs. 3C and D). Consistent with this smaller weight gap, the rate of growth of female *Runx2*$^{+/-}$ *Grg5*$^{-/-}$ mice was greater than that of wild-type mice after 5 weeks of postnatal growth. After 2–3 months, the weight and size of the female *Runx2*$^{+/-}$ *Grg5*$^{-/-}$ mice were similar to those of wild-type littermates (data not shown).

In summary, the compound *Runx2*$^{+/-}$ *Grg5*$^{-/-}$ mice exhibited a dramatic phenotype of reduced growth. Inspection of the growth curves, which combine the data of all individuals within each genotype, clearly shows that the growth rate reduction in *Runx2*$^{+/-}$ *Grg5*$^{-/-}$ mice is greater than would be expected if Runx2 and Grg5 contributed independently to growth (Fig. 3). Therefore, the results strongly suggest that Runx2 and Grg5 interact genetically in vivo and regulate postnatal growth in mice. The observations on skeletal size and bone density also suggest a specific effect on skeletal development and growth (Figs. 4A and B).

Delayed cranial suture closure in Runx2$^{+/-}$ *Grg5*$^{-/-}$ *mice*

Delayed closure of cranial sutures and hypoplastic clavicles are prominent features of cleidocranial dysplasia (CCD) in humans and mice resulting from haploinsufficiency of *Runx2* (Huang et al., 1997; Komori et al., 1997; Mundlos et al., 1997; Otto et al., 1997). Cranial sutures and clavicles in *Grg5* null mice are not affected. The defect in the fontanel closure in *Runx2*$^{+/-}$ *Grg5*$^{-/-}$ mice was more severe than in heterozygous *Runx2* mice as would be expected if the activity of Runx2 was reduced in the absence of Grg5 (Fig. 4C). On the other hand, there was no discernible difference between the hypoplastic clavicles of *Runx2* heterozygotes and those of *Runx2* $^{+/-}$ Grg5$^{-/-}$ mice. Because the clavicles of *Runx2* heterozygous mice completely lack the medial cartilaginous anlage (Huang et al., 1997), it was not surprising that the lack of Grg5 did not exacerbate this defect.

Calvarial bones are formed by intramembranous ossification. The more marked widening of the fontanels in *Runx2*$^{+/-}$ *Grg5*$^{-/-}$ mice (as compared to Runx2$^{+/-}$ mice) suggests that osteoblastic activity is reduced (Opperman, 2000). To test this possibility, we isolated primary osteoblasts from the calvaria of newborn mice of various genotypes to examine osteoblastic activity in vitro (Wang et al., 2002). Among osteoblast cultures from wild-type, *Runx2* heterozygous, *Grg5* null, or *Runx2*$^{+/-}$ *Grg5*$^{-/-}$ mice, no differences were detected in their ability to form mineralized

nodules (data not shown). Therefore, the delay in fontanel closure in *Runx2*$^{+/-}$*Grg5*$^{-/-}$ mice may result from a decrease in the number of differentiated osteoblasts rather than a decreased ability of each osteoblast to form bone.

Growth plate defects in Runx2$^{+/-}$ *Grg5*$^{-/-}$ *mice*

The small skeletons of *Runx2*$^{+/-}$ *Grg5*$^{-/-}$ mice suggested a growth plate defect as we have previously demonstrated in the study of *Grg5* null mice (Wang et al., 2002). Histological analysis of the growth plates of tibia and humerus was therefore carried out using decalcified sections. By comparing these bones in *Runx2*$^{+/+}$ *Grg5*$^{+/-}$, *Runx2*$^{+/-}$ *Grg5*$^{+/+}$, *Runx2*$^{+/+}$ *Grg5*$^{-/-}$, and *Runx2*$^{+/-}$ *Grg5*$^{-/-}$ mice, a striking reduction in the overall height of the growth plates as well as a reduction in the amount of trabecular bone subjacent to the growth plates was found in *Runx2*$^{+/-}$ *Grg5*$^{-/-}$ mice (Figs. 5A–H). This abnormality was clearly more severe than the defect seen in Runx2$^{+/+}$ Grg5$^{-/-}$ mice. In Runx2$^{+/-}$ Grg5$^{-/-}$ mice, the zone of hypertrophic chondrocytes was clearly thinner than in the controls (Figs. 5E–H). Although a mild growth defect (body weight) was observed in *Runx2* heterozygous mice (Fig. 3), no obvious histological growth plate defect could be seen in these mice (Figs. 5B and F).

We used immunostaining for proliferating cellular nuclear antigen (PCNA) to compare proliferating chondrocytes in tibial growth plates. In our previous study, the percentage of PCNA-positive cells in affected *Grg5* null mice was reduced to about 75% of wild-type mice (Wang et al., 2002). In *Runx2*$^{+/-}$ *Grg5*$^{-/-}$ mice, this percentage was even more drastically reduced to 35–45% of wild-type mice (Figs. 5I–L). Moreover, PCNA staining allowed us to distinguish the proliferative zone of the growth plate from the resting and hypertrophic zones. We could clearly determine that the reduced thickness of the growth plate in Runx2$^{+/+}$ Grg5$^{-/-}$ mice was due to a reduction in the thickness of the proliferative as well as the hypertrophic zones (Figs. 5I–L). Immunostaining for collagen type II confirmed that the hypertrophic zone of chondrocytes in *Runx2*$^{+/-}$ *Grg5*$^{-/-}$ mice was thinner than in the controls (Figs. 5M–P). Similar observations were made for the growth plates of humerus (data not shown).

Reduced Ihh signaling in Runx2$^{+/-}$ *Grg5*$^{-/-}$ *mice*

Previously published data on the role of Runx2 in chondrocyte differentiation suggest that it is involved in regulating Ihh signaling (Inada et al., 1999; Kim et al., 1999; St-Jacques and Hammerschmidt, 1999; Takeda et al., 2001). In our study of *Grg5* null mice, we found that the growth plate defect in *Grg5* null mice was associated with reduced Ihh signaling (Wang et al., 2002). To examine Ihh signaling in the growth plates of *Runx2*$^{+/-}$ *Grg5*$^{-/-}$ mice, we performed in situ hybridization for *Col10a1* and *Ihh* (Fig. 6). Expression of *Col10a1* was similar in all mice (Figs. 6A–D). The Ihh signal in the growth plates of both *Runx2*$^{+/-}$ *Grg5*$^{-/-}$ and their *Grg5* null littermates was reduced compared with *Runx2*$^{+/+}$ *Grg5*$^{+/-}$ and *Runx2*$^{+/-}$ *Grg5*$^{+/+}$ control animals (Figs. 6E–H), but this reduction was more drastic in *Runx2*$^{+/-}$ *Grg5*$^{-/-}$ mice. We used immunohistochemistry to further investigate the expression of Ihh and other molecules involved in Ihh signaling such as Ptc, Smo, and PTHrP. In contrast to the clear and robust Ihh and Smo immunostaining in wild-type or *Runx2* heterozygous sections, Ihh-positive or Smo-positive prehypertrophic chondrocytes were significantly reduced in *Grg5* null mice while those in the *Runx2*$^{+/-}$ *Grg5*$^{-/-}$ sections were barely detectable (Fig. 7A). To semiquantitatively measure Ihh expression in growth plates, Ihh-positive prehypertrophic chondrocytes were counted and the numbers of such cells were compared between the different genotypes (Fig. 7B). Despite the fact that the number of Ihh-positive cells in Grg5 null mice was significantly reduced (about 40% of *Runx2*$^{+/+}$ *Grg5*$^{+/-}$ mice), a more drastic reduction was seen in *Runx2*$^{+/-}$ *Grg5*$^{-/-}$ mice (about 20% of *Runx2*$^{+/+}$ *Grg5*$^{+/-}$ mice). Ptc protein was also reduced in a similar pattern. We also performed immunostaining for PTHrP because it is a downstream target of Ihh signaling (Lanske et al., 1996; St-Jacques and Hammerschmidt, 1999; Vortkamp et al., 1996). PTHrP expression in *Runx2*$^{+/-}$ *Grg5*$^{-/-}$ growth plates was undetectable and there was a dramatic reduction in *Grg5* null growth plates compared to wild-type controls (data not shown). Therefore, we conclude that reduced Ihh signaling is a major cause of the severe growth plate defect in *Runx2*$^{+/-}$ *Grg5*$^{-/-}$ mice.

In an attempt to understand why trabecular bone formation is so dramatically reduced subjacent to the growth plates of *Runx2*$^{+/-}$ *Grg5*$^{-/-}$ mice, we examined osteoblasts and osteoclasts in tissue sections by assaying for *Col1a1* mRNA expression and tartrate-resistant acid phosphatase (TRAP), respectively. No increase in the number of TRAP-positive osteoclasts was found subjacent to the growth plates of *Runx2*$^{+/-}$ *Grg5*$^{-/-}$ mice compared with their control littermates (data not shown). Using in situ hybridization for *Col1a1*, a marker for osteoblasts, the total amount of *Col1a1* signal in *Runx2*$^{+/-}$ *Grg5*$^{-/-}$ mice was drastically reduced, but the intensity of the signal per cell was similar among all the different genotypes (Figs. 6I–L). Therefore, we conclude, as we previously did for *Grg5* null mice, that osteoblastic recruitment under the defective growth plates of *Runx2*$^{+/-}$ *Grg5*$^{-/-}$ mice is reduced, leading to the osteopenic phenotype.

Discussion

Grg5 is a coactivator of Runx2

Grg5 is one of several proteins that have been shown to bind to the C-terminal region of Runx2 in vitro. These proteins can act as either coactivators or corepressors and include Grgs/Tles, Hes-1 (Hairy/Enhancer of split 1), Moz

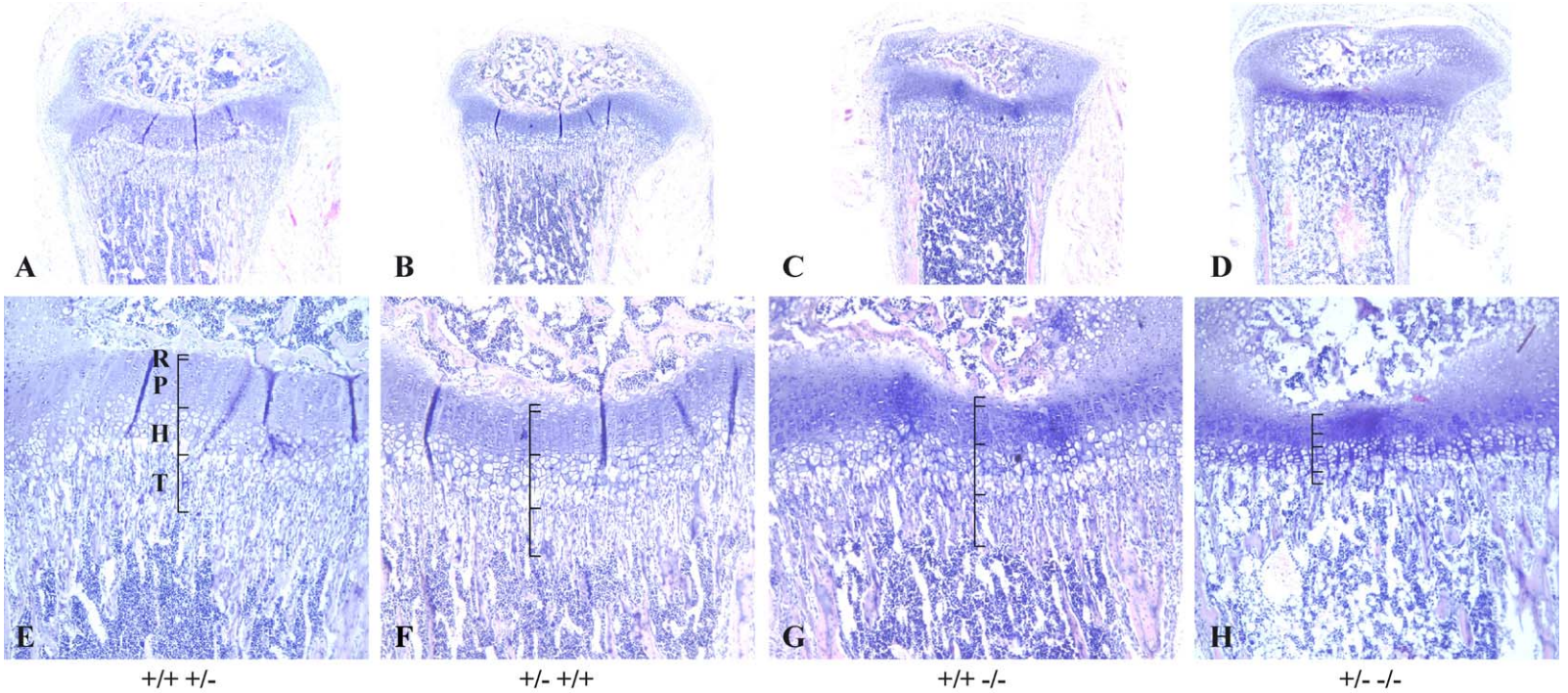

Fig. 5. Histology of proximal tibial growth plates from 3-week-old mice with the genotypes *Runx2*$^{+/+}$ *Grg*$^{+/-}$, *Runx2*$^{+/-}$ *Grg5*$^{+/+}$, *Runx2*$^{+/+}$ *Grg5*$^{-/-}$, and *Runx2*$^{+/-}$ *Grg5*$^{-/-}$. (A–H) Hematoxylin and eosin staining of decalcified growth plate sections. Based on chondrocyte morphology, a growth plate can be divided into resting (R), proliferative (P), and hypertrophic zones (H). These zones, as well as the region of trabecular bone (T) below the growth plate, are indicated along the vertical lines in E–H and labeled in E. Note the expansion of the resting zone and the thinner zones of proliferation and hypertrophy in the *Runx2*$^{+/-}$ *Grg5*$^{-/}$growth plate. (I–L) PCNA immunostaining in growth plates. (M–P) Collagen type II immunostaining.

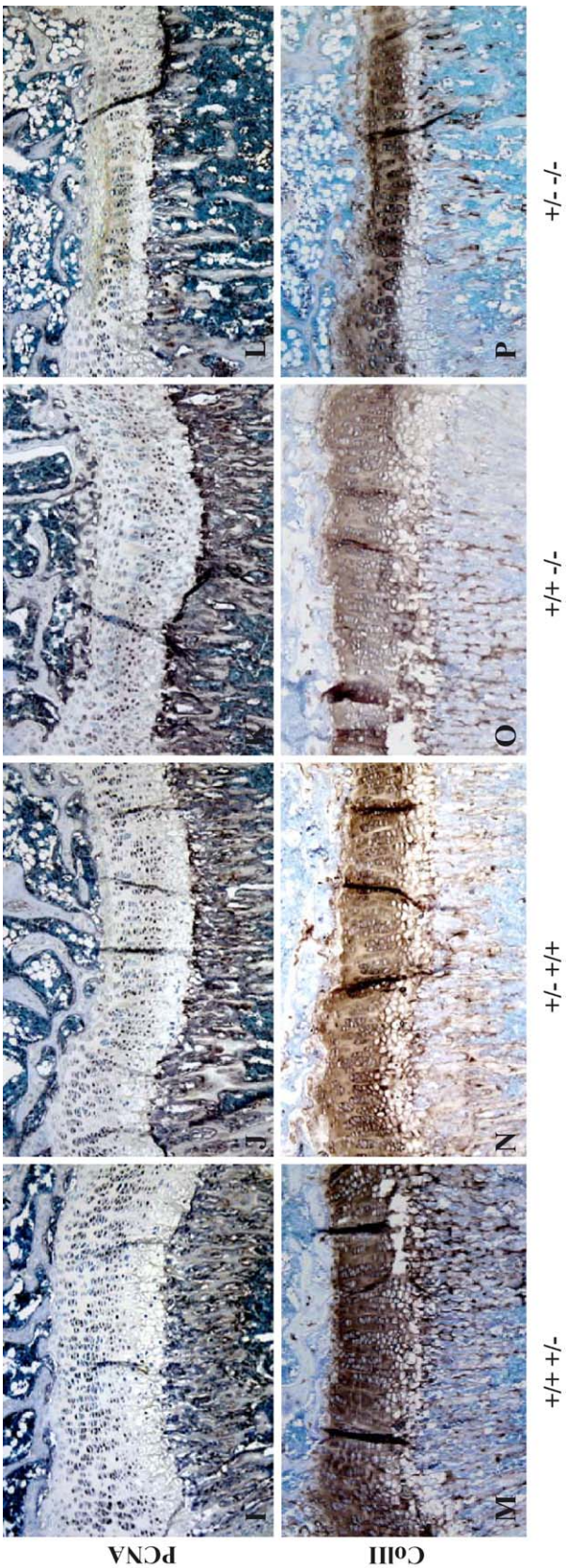

Fig. 5 (*continued*).

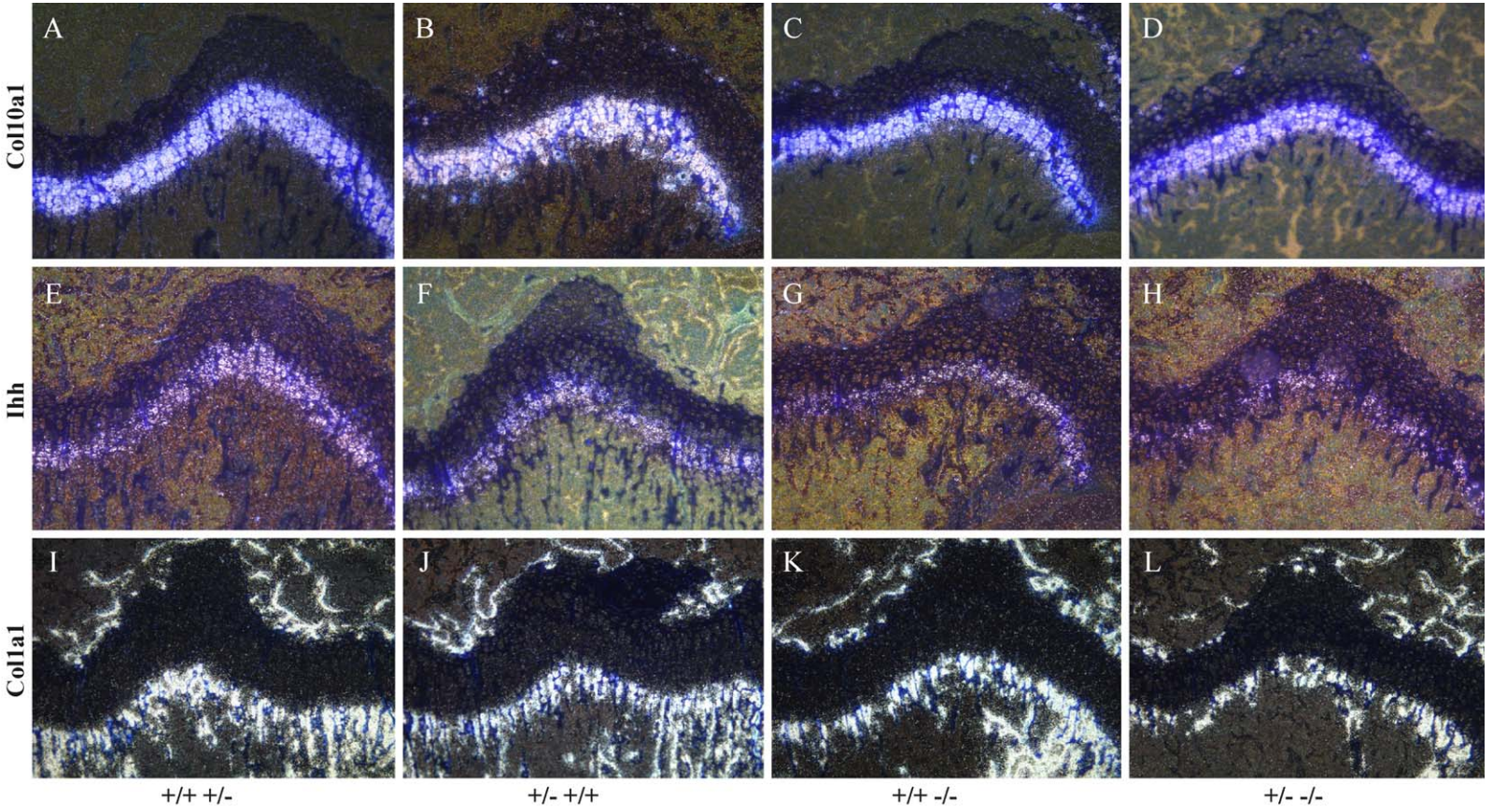

Fig. 6. Expression of molecular markers in growth plates from humeri of 3-week-old mice with genotypes *Runx2*$^{+/+}$ *Grg*$^{+/-}$, *Runx2*$^{+/-}$ *Grg5*$^{+/+}$, *Runx2*$^{+/+}$ *Grg5*$^{-/-}$, and *Runx2*$^{+/-}$ *Grg5*$^{-/-}$. (A–D) In situ hybridization of *Col10a1*. No significant difference in *Col10a1* expression in hypertrophic chondrocytes is seen between the different genotypes. (E–H) In situ hybridization of *Ihh*. Reduced Ihh expression in *Runx2*$^{+/-}$ *Grg5*$^{-/-}$ section is more dramatic than that in the *Grg5* null section. Note that the *Runx2*$^{+/+}$ *Grg5*$^{-/-}$ section is from a severely affected *Grg5* null mouse. (I–L) In situ hybridization of *Col1a1* in trabecular bone under the growth plates and in the secondary ossification centers above. The amount of *Col1a1* mRNA is dramatically reduced in the *Runx2*$^{+/-}$ *Grg5*$^{-/-}$ section.

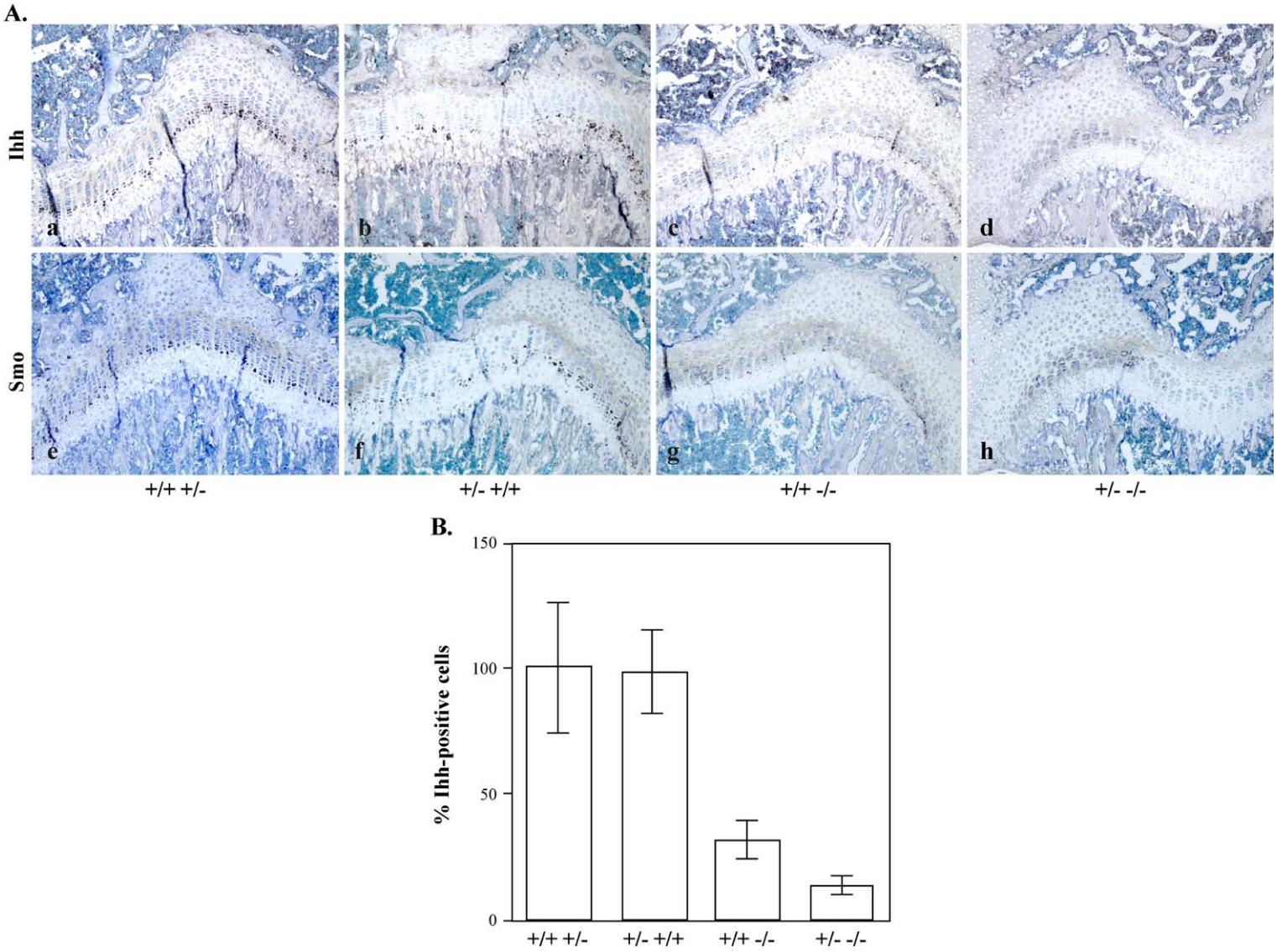

Fig. 7. Ihh signaling in the proximal growth plates of humeri in *Runx2*$^{+/-}$ *Grg5*$^{-/-}$ mice. (A, a–d) Ihh protein detected by immunostaining using antibodies against *hedgehog* proteins. Ihh-positive pre-hypertrophic chondrocytes in wild-type or *Runx2* heterozygous mice occupy 2–3 cell layers in the growth plates. In contrast, barely one layer of Ihh-positive cells is present in *Runx2*$^{+/+}$ *Grg5*$^{-/-}$ mice, and Ihh-positive cells are undetectable in *Runx2*$^{+/-}$ *Grg5*$^{-/-}$ mice. (e–h) Similar immunostaining results are shown for the Ihh receptor component Smo. (B) Bar graph of relative percentage of Ihh-positive pre-hypertrophic chondrocytes in the growth plates of *Runx2*$^{+/+}$ *Grg*$^{+/-}$, *Runx2*$^{+/-}$ *Grg5*$^{+/+}$, *Runx2*$^{+/+}$ *Grg5*$^{-/-}$, and *Runx2*$^{+/-}$ *Grg5*$^{-/-}$ mice (sections from three mice were analyzed for each genotype). Standard deviations are indicated by error bars. The number of Ihh-positive cells in *Runx2*$^{+/-}$ *Grg5*$^{-/-}$ mice was significantly reduced in comparison with that of *Runx2*$^{+/+}$ *Grg5*$^{-/-}$ mice.

and Morf (histone acetyltransferases), HDAC6 (histone deacetylase), and Taz (transcriptional coactivator with PDZ motif) (Cui et al., 2003; Hess et al., 2001; Javed et al., 2000; McLarren et al., 2000; Pelletier et al., 2002; Shirakabe et al., 2001; Tahirov et al., 2001; Westendorf et al., 2002). In vitro experiments show that Runx2 in association with different members of this group of proteins can act as a transcriptional activator or repressor. In the case of Grgs, the long forms in general act as corepressors, whereas Grg5, a short form, is a coactivator for Runx2. The full-length Grg5 behaved differently from the truncated version of Grg5, Grg5ΔN27, isolated in the yeast two-hybrid screen as a Runx2-interacting protein, on proteins encoded by three Runx2 deletion constructs, ΔN1–48, ΔN1–94, and ΔC516–528 (Fig. 2A). This leads us to hypothesize that the first 27 amino acid residues of Grg5 may block Grg5 coactivating activity. This blocking activity can be overcome either by deleting the N-terminal 27 amino acid region (as in Grg5ΔN27) or by an interaction requiring both the N- and C-terminal regions of Runx2. The N-terminal 27 amino acid residues in Grg5 may function as a specific activation or interaction "switch". Alternatively, its nonspecific interference with activation of Runx2 lacking N- or C-terminal regions may be nonspecific. Further studies are clearly needed to address these possibilities.

Effects of Runx2 and Grg5 deficiency on body weight and skeletal growth

Patients with cleidocranial dysplasia, heterozygous for loss-of-function mutations in *Runx2*, tend to have a short stature, and *Runx2* null mice are notably smaller than their heterozygous and wild-type littermates. *Runx2*$^{+/-}$ *Grg5*$^{+/+}$ mice in this study gained weight more slowly than their wild-type littermates during the first 6 weeks after birth (Fig. 3). It has already been documented that *Grg5* null mice have a growth delay (see also Fig. 3) which in about 50% of the mice results in a runted phenotype (Wang et al., 2002), while growth curves for heterozygous *Grg5*$^{+/-}$ mice were indistinguishable from those of wild-type mice. The growth curves clearly indicate that the combination of heterozygous loss of Runx2 activity and complete lack of Grg5 function results in a growth deficiency that is greater than would be expected if Runx2 and Grg5 contributed independently to growth. This compound genotype caused a severe growth plate abnormality that likely contributed to the reduced size and density of the skeleton in the mutant mice.

We do not wish to imply that the effects of *Grg5* deficiency on the overall growth and on the skeleton are entirely secondary to a reduction in the activity of Runx2. Grg5 is ubiquitously expressed and has been shown to bind Tcfs in vitro and regulate their activities (Brantjes et al., 2001; Cavallo et al., 1998; Roose et al., 1998). In addition, *Grg5* deficiency has been reported to cause pituitary abnormalities and growth insufficiency based on the loss of its normal interaction with Tcf4 (Brinkmeier et al., 2003). Therefore, the effects described here on overall growth, skeletal growth, and growth plate structure are likely to involve relatively complex mechanisms. For example, because Tcf4 has shown to be expressed in hypertrophic chondrocytes and Lef1 by cells in the perichondrium (Hartmann and Tabin, 2000), Grg5 may modulate the activity of Tcf4/Lef1 in osteoblasts and chondrocytes. Furthermore, Wnt molecules, such as Wnt5a and Wnt5b, are known to play important roles in chondrocyte proliferation and differentiation in growth plates (Hartmann and Tabin, 2000; Yang et al., 2003); and it is likely that Tcf4/Lef1 represents downstream targets in these Wnt signaling pathways (Huelsken and Birchmeier, 2001). Therefore, Grg5 may function in chondrocytes of long bone growth plates as a versatile coactivator of various transcription factors including Runx2 and Tcf4.

The reduced activity of Runx2 in the absence of Grg5 leads to proliferative and hypertrophic zones of reduced height in postnatal growth plates of *Runx2*$^{+/-}$ *Grg5*$^{-/-}$ mice (Fig. 5). Although *Runx2* null embryos have short limbs, Runx2 effects on chondrocyte proliferation have not been clearly established (Inada et al., 1999; Kim et al., 1999). Our data indicate that Runx2 unquestionably plays a role in controlling chondrocyte proliferation. Interestingly, the resting zone of the growth plates in *Runx2*$^{+/-}$ *Grg5*$^{-/-}$ mice was expanded (Fig. 5). This increased "reserve" of chondrocytes may explain why the overall growth of *Runx2*$^{+/-}$ *Grg5*$^{-/-}$ mice somehow recovered with age (Fig. 5). What triggers this recovery is not known, but we speculate that estrogen–estrogen receptor (ER) signaling may contribute to this recovery concomitant with sexual maturation. The growth rates of the female *Grg5* null (*Runx2* wild-type) and *Runx2*$^{+/-}$ *Grg5*$^{-/-}$ mice were higher than those of wild-type mice after 4–5 weeks of age, whereas the male *Grg5* null (*Runx2* wild-type) and *Runx2*$^{+/-}$ *Grg5*$^{-/-}$ mice maintained similar or even lower growth rates (Fig. 3). Estrogen receptor-α (ERα) is present in both osteoblasts and chondrocytes (Nilsson et al., 2002; Riggs et al., 2002). Estrogen treatment of osteoblastic cells in culture enhances *Runx2* expression. The nuclear steroid receptor ERα interacts with Runx2 when their DNA binding sites are in proximity (McCarthy et al., 2003). Furthermore, high levels of estrogen in mice increase the number of Runx2-positive osteoblasts (Plant and Tobias, 2001, 2002; Plant et al., 2002). Conversely, ERα null mice have shorter and smaller long bones than wild-type mice (Couse and Korach, 1999; Hewitt and Korach, 2002; Vidal et al., 2000; Weise et al., 2001).

Ihh is a target of Runx2 in growth plate chondrocytes

Ihh is a major regulator of bone development and growth. It coordinates chondrocyte proliferation, chondrocyte differentiation, and osteoblast differentiation (Kronenberg, 2003). Several lines of evidence suggest that Ihh in the prehypertrophic chondrocytes is a target of Runx2 in growth plates. First, no *Ihh* expression is detected in chondrocytes of

proximal limb cartilages in *Runx2* null mice, and the expression of Ihh is markedly reduced in the distal limbs where chondrocyte hypertrophy occurs (Inada et al., 1999; Kim et al., 1999). Second, overexpression of *Runx2* in chondrocytes prematurely induces *Ihh* expression in ribs and promotes chondrocyte hypertrophy (Takeda et al., 2001; Ueta et al., 2001). Third, *Runx2* expression in chondrocytes is maintained in *Ihh* null mice (St-Jacques and Hammerschmidt, 1999). Furthermore, *Runx2* mRNA is upregulated in prehypertrophic chondrocytes where *Ihh* expression is localized. The results of the present study suggest that the Grg5 effect on *Ihh* expression is mediated by Runx2. Reduced Runx2 activity ($Runx2^{+/-}$) in the absence of Grg5 leads to severely reduced *Ihh* expression and signaling in growth plates compared with mice with Runx2 deficiency and normal Grg5 function. The precise pathway for Runx2 control of *Ihh* expression in growth plate chondrocytes awaits further study.

In summary, we have provided in vitro and in vivo evidence that Grg5 interacts with Runx2 and acts as a positive regulator of Runx2. A severe postnatal growth defect is seen in $Runx2^{+/-}$ $Grg5^{-/-}$ mice that is correlated with defects in both membranous and endochondral bone formation. The long bones have growth plate defects with narrowed proliferative and hypertrophic zones and expanded resting zones. These defects are associated with reduced *Ihh* expression and reduced Ihh signaling. We conclude that reduced Runx2 activity in the absence of Grg5 activity in the chondrocytes of growth plate leads to defects caused by reduced Ihh expression.

Acknowledgments

We thank Drs. M. J. Owen and T. Gridley for providing Runx2 and Grg5 mutant mice, respectively. We are indebted to Yulia Pittel for excellent secretarial assistance. W. F. W. was supported in part by a training grant from Harvard School of Dental Medicine/Massachusetts Institute of Technology. This work was supported by NIH grants AR36819 and AR36820 (to B. R. O.) and AR045548 (to G. K.).

References

Adya, N., Castilla, L.H., Liu, P.P., 2000. Function of CBFbeta/Bro proteins. Semin. Cell Dev. Biol. 11, 361–368.

Aronson, B.D., Fisher, A.L., Blechman, K., Caudy, M., Gergen, J.P., 1997. Groucho-dependent and -independent repression activities of Runt domain proteins. Mol. Cell. Biol. 17, 5581–5587.

Brantjes, H., Roose, J., van De Wetering, M., Clevers, H., 2001. All Tcf HMG box transcription factors interact with Groucho-related co-repressors. Nucleic Acids Res. 29, 1410–1419.

Brinkmeier, M.L., Potok, M.A., Cha, K.B., Gridley, T., Stifani, S., Meeldijk, J., Clevers, H., Camper, S.A., 2003. TCF4 and groucho-related genes influence pituitary growth and development. Mol. Endocrinol. 17, 2152–2161.

Castilla, L.H., Wijmenga, C., Wang, Q., Stacy, T., Speck, N.A., Eckhaus, M., Marin-Padilla, M., Collins, F.S., Wynshaw-Boris, A., Liu, P.P., 1996. Failure of embryonic hematopoiesis and lethal hemorrhages in mouse embryos heterozygous for a knocked-in leukemia gene CBFB-MYH11. Cell 87, 687–696.

Cavallo, R.A., Cox, R.T., Moline, M.M., Roose, J., Polevoy, G.A., Clevers, H., Peifer, M., Bejsovec, A., 1998. *Drosophila* Tcf and Groucho interact to repress Wingless signalling activity. Nature 395, 604–608.

Chen, G., Courey, A.J., 2000. Groucho/TLE family proteins and transcriptional repression. Gene 249, 1–16.

Couse, J.F., Korach, K.S., 1999. Estrogen receptor null mice: what have we learned and where will they lead us? Endocr. Rev. 20, 358–417.

Cui, C.B., Cooper, L.F., Yang, X., Karsenty, G., Aukhil, I., 2003. Transcriptional coactivation of bone-specific transcription factor Cbfa1 by TAZ. Mol. Cell. Biol. 23, 1004–1013.

Ducy, P., Zhang, R., Geoffroy, V., Ridall, A.L., Karsenty, G., 1997. Osf2/Cbfa1 a transcriptional activator of osteoblast differentiation [see comments]. Cell 89, 747–754.

Ducy, P., Starbuck, M., Priemel, M., Shen, J., Pinero, G., Geoffroy, V., Amling, M., Karsenty, G., 1999. A Cbfa1-dependent genetic pathway controls bone formation beyond embryonic development. Genes Dev. 13, 1025–1036.

Geoffroy, V., Kneissel, M., Fournier, B., Boyde, A., Matthias, P., 2002. High bone resorption in adult aging transgenic mice overexpressing cbfa1/runx2 in cells of the osteoblastic lineage. Mol. Cell. Biol. 22, 6222–6233.

Guo, W.H., Weng, L.Q., Ito, K., Chen, L.F., Nakanishi, H., Tatematsu, M., Ito, Y., 2002. Inhibition of growth of mouse gastric cancer cells by Runx3, a novel tumor suppressor. Oncogene 21, 8351–8355.

Hartmann, C., Tabin, C.J., 2000. Dual roles of Wnt signaling during chondrogenesis in the chicken limb. Development 127, 3141–3159.

Hess, J., Porte, D., Munz, C., Angel, P., 2001. AP-1 and Cbfa/runt physically interact and regulate parathyroid hormone-dependent MMP13 expression in osteoblasts through a new osteoblast-specific element 2/AP-1 composite element. J. Biol. Chem. 276, 20029–20038.

Hewitt, S.C., Korach, K.S., 2002. Estrogen receptors: structure, mechanisms and function. Rev. Endocr. Metab. Disord. 3, 193–200.

Huang, L.F., Fukai, N., Selby, P.B., Olsen, B.R., Mundlos, S., 1997. Mouse clavicular development: analysis of wild-type and cleidocranial dysplasia mutant mice. Dev. Dyn. 210, 33–40.

Huelsken, J., Birchmeier, W., 2001. New aspects of Wnt signaling pathways in higher vertebrates. Curr. Opin. Genet. Dev. 11, 547–553.

Inada, M., Yasui, T., Nomura, S., Miyake, S., Deguchi, K., Himeno, M., Sato, M., Yamagiwa, H., Kimura, T., Yasui, N., Ochi, T., Endo, N., Kitamura, Y., Kishimoto, T., Komori, T., 1999. Maturational disturbance of chondrocytes in Cbfa1-deficient mice. Dev. Dyn. 214, 279–290.

Inoue, K., Ozaki, S., Shiga, T., Ito, K., Masuda, T., Okado, N., Iseda, T., Kawaguchi, S., Ogawa, M., Bae, S.C., Yamashita, N., Itohara, S., Kudo, N., Ito, Y., 2002. Runx3 controls the axonal projection of proprioceptive dorsal root ganglion neurons. Nat. Neurosci. 5, 946–954.

Javed, A., Guo, B., Hiebert, S., Choi, J.Y., Green, J., Zhao, S.C., Osborne, M.A., Stifani, S., Stein, J.L., Lian, J.B., van Wijnen, A.J., Stein, G.S., 2000. Groucho/TLE/R-esp proteins associate with the nuclear matrix and repress RUNX (CBF(alpha)/AML/PEBP2(alpha)) dependent activation of tissue-specific gene transcription. J. Cell Sci. 113, 2221–2231.

Karsenty, G., Wagner, E.F., 2002. Reaching a genetic and molecular understanding of skeletal development. Dev. Cell 2, 389–406.

Kim, I.S., Otto, F., Zabel, B., Mundlos, S., 1999. Regulation of chondrocyte differentiation by Cbfa1. Mech. Dev. 80, 159–170.

Komori, T., Yagi, H., Nomura, S., Yamaguchi, A., Sasaki, K., Deguchi, K., Shimizu, Y., Bronson, R.T., Gao, Y.H., Inada, M., Sato, M., Okamoto, R., Kitamura, Y., Yoshiki, S., Kishimoto, T., 1997. Targeted disruption of Cbfa1 results in a complete lack of bone formation owing to maturational arrest of osteoblasts [see comments]. Cell 89, 755–764.

Kronenberg, H.M., 2003. Developmental regulation of the growth plate. Nature 423, 332–336.

Kundu, M., Chen, A., Anderson, S., Kirby, M., Xu, L., Castilla, L.H.,

Bodine, D., Liu, P.P., 2002. Role of Cbfb in hematopoiesis and perturbations resulting from expression of the leukemogenic fusion gene Cbfb-MYH11. Blood 100, 2449–2456.

Lanske, B., Karaplis, A.C., Lee, K., Luz, A., Vortkamp, A., Pirro, A., Karperien, M., Defize, L.H., Ho, C., Mulligan, R.C., Abou-Samra, A.B., Juppner, H., Segre, G.V., Kronenberg, H.M., 1996. PTH/PTHrP receptor in early development and Indian hedgehog-regulated bone growth. Science 273, 663–666.

Leon, C., Lobe, C.G., 1997. Grg3, a murine Groucho-related gene, is expressed in the developing nervous system and in mesenchyme-induced epithelial structures. Dev. Dyn. 208, 11–24.

Levanon, D., Goldstein, R.E., Bernstein, Y., Tang, H., Goldenberg, D., Stifani, S., Paroush, Z., Groner, Y., 1998. Transcriptional repression by AML1 and LEF-1 is mediated by the TLE/Groucho corepressors. Proc. Natl. Acad. Sci. U. S. A. 95, 11590–11595.

Levanon, D., Bettoun, D., Harris-Cerruti, C., Woolf, E., Negreanu, V., Eilam, R., Bernstein, Y., Goldenberg, D., Xiao, C., Fliegauf, M., Kremer, E., Otto, F., Brenner, O., Lev-Tov, A., Groner, Y., 2002. The Runx3 transcription factor regulates development and survival of TrkC dorsal root ganglia neurons. EMBO J. 21, 3454–3463.

Li, Q.L., Ito, K., Sakakura, C., Fukamachi, H., Inoue, K., Chi, X.Z., Lee, K.Y., Nomura, S., Lee, C.W., Han, S.B., Kim, H.M., Kim, W.J., Yamamoto, H., Yamashita, N., Yano, T., Ikeda, T., Itohara, S., Inazawa, J., Abe, T., Hagiwara, A., Yamagishi, H., Ooe, A., Kaneda, A., Sugimura, T., Ushijima, T., Bae, S.C., Ito, Y., 2002. Causal relationship between the loss of RUNX3 expression and gastric cancer. Cell 109, 113–124.

Liu, W., Toyosawa, S., Furuichi, T., Kanatani, N., Yoshida, C., Liu, Y., Himeno, M., Narai, S., Yamaguchi, A., Komori, T., 2001. Overexpression of Cbfa1 in osteoblasts inhibits osteoblast maturation and causes osteopenia with multiple fractures. J. Cell Biol. 155, 157–166.

Mallo, M., Franco del Amo, F., Gridley, T., 1993. Cloning and developmental expression of Grg, a mouse gene related to the groucho transcript of the *Drosophila* Enhancer of split complex. Mech. Dev. 42, 67–76.

Mallo, M., Gendron-Maguire, M., Harbison, M.L., Gridley, T., 1995. Protein characterization and targeted disruption of Grg, a mouse gene related to the groucho transcript of the *Drosophila* Enhancer of split complex. Dev. Dyn. 204, 338–347.

McCarthy, T.L., Chang, W.Z., Liu, Y., Centrella, M., 2003. Runx2 integrates estrogen activity in osteoblasts. J. Biol. Chem. 278, 43121–43129.

McLarren, K.W., Lo, R., Grbavec, D., Thirunavukkarasu, K., Karsenty, G., Stifani, S., 2000. The mammalian basic helix loop helix protein HES-1 binds to and modulates the transactivating function of the runt-related factor Cbfa1. J. Biol. Chem. 275, 530–538.

Miller, J., Horner, A., Stacy, T., Lowrey, C., Lian, J.B., Stein, G., Nuckolls, G.H., Speck, N.A., 2002. The core-binding factor beta subunit is required for bone formation and hematopoietic maturation. Nat. Genet. 32, 645–649.

Miyasaka, H., Choudhury, B.K., Hou, E.W., Li, S.S., 1993. Molecular cloning and expression of mouse and human cDNA encoding AES and ESG proteins with strong similarity to *Drosophila* enhancer of split groucho protein. Eur. J. Biochem. 216, 343–352.

Mundlos, S., Otto, F., Mundlos, C., Mulliken, J.B., Aylsworth, A.S., Albright, S., Lindhout, D., Cole, W.G., Henn, W., Knoll, J.H., Owen, M.J., Mertelsmann, R., Zabel, B.U., Olsen, B.R., 1997. Mutations involving the transcription factor CBFA1 cause cleidocranial dysplasia [see comments]. Cell 89, 773–779.

Nilsson, O., Abad, V., Chrysis, D., Ritzen, E.M., Savendahl, L., Baron, J., 2002. Estrogen receptor-alpha and -beta are expressed throughout postnatal development in the rat and rabbit growth plate. J. Endocrinol. 173, 407–414.

Olsen, B.R., Reginato, A.M., Wang, W., 2000. Bone development. Annu. Rev. Cell Dev. Biol. 16, 191–220.

Opperman, L.A., 2000. Cranial sutures as intramembranous bone growth sites. Dev. Dyn. 219, 472–485.

Otto, F., Thornell, A.P., Crompton, T., Denzel, A., Gilmour, K.C., Rosewell, I.R., Stamp, G.W., Beddington, R.S., Mundlos, S., Olsen, B.R., Selby, P.B., Owen, M.J., 1997. Cbfa1, a candidate gene for cleidocranial dysplasia syndrome, is essential for osteoblast differentiation and bone development [see comments]. Cell 89, 765–771.

Otto, F., Kanegane, H., Mundlos, S., 2002. Mutations in the RUNX2 gene in patients with cleidocranial dysplasia. Hum. Mutat. 19, 209–216.

Pelletier, N., Champagne, N., Stifani, S., Yang, X.J., 2002. MOZ and MORF histone acetyltransferases interact with the Runt-domain transcription factor Runx2. Oncogene 21, 2729–2740.

Pinheiro, J.C., Bates, D.M., 2000. Nonlinear mixed-effects models; basic concepts and motivating examples. Mixed-Effects Models in S and S-PLUS. Springer, New York, pp. 273–305.

Plant, A., Tobias, J.H., 2001. Characterisation of the temporal sequence of osteoblast gene expression during estrogen-induced osteogenesis in female mice. J. Cell. Biochem. 82, 683–691.

Plant, A., Tobias, J.H., 2002. Increased bone morphogenetic protein-6 expression in mouse long bones after estrogen administration. J. Bone Miner. Res. 17, 782–790.

Plant, A., Samuels, A., Perry, M.J., Colley, S., Gibson, R., Tobias, J.H., 2002. Estrogen-induced osteogenesis in mice is associated with the appearance of Cbfa1-expressing bone marrow cells. J. Cell. Biochem. 84, 285–294.

Riggs, B.L., Khosla, S., Melton III, L.J., 2002. Sex steroids and the construction and conservation of the adult skeleton. Endocr. Rev. 23, 279–302.

Roose, J., Molenaar, M., Peterson, J., Hurenkamp, J., Brantjes, H., Moerer, P., van de Wetering, M., Destree, O., Clevers, H., 1998. The *Xenopus* Wnt effector XTcf-3 interacts with Groucho-related transcriptional repressors. Nature 395, 608–612.

Sambrook, J., Fritsch, E.F., Maniatis, T., 1989. Molecular Cloning, A Laboratory Manual. Cold Spring Harbor Laboratory Press, New York.

Shirakabe, K., Terasawa, K., Miyama, K., Shibuya, H., Nishida, E., 2001. Regulation of the activity of the transcription factor Runx2 by two homeobox proteins, Msx2 and Dlx5. Genes Cells 6, 851–856.

Speck, N.A., Stacy, T., Wang, Q., North, T., Gu, T.L., Miller, J., Binder, M., Marin-Padilla, M., 1999. Core-binding factor: a central player in hematopoiesis and leukemia. Cancer Res. 59, 1789s–1793s.

Stifani, S., Blaumueller, C.M., Redhead, N.J., Hill, R.E., Artavanis-Tsakonas, S., 1992. Human homologs of a *Drosophila* Enhancer of split gene product define a novel family of nuclear proteins [published erratum appears in Nat Genet 1992 Dec;2(4):343]. Nat. Genet. 2, 119–127.

St-Jacques, B., Hammerschmidt, M., McMahon, A.P., 1999. Indian hedgehog signaling regulates proliferation and differentiation of chondrocytes and is essential for bone formation. Genes Dev. 13, 2072–2086.

Tahirov, T.H., Inoue-Bungo, T., Morii, H., Fujikawa, A., Sasaki, M., Kimura, K., Shiina, M., Sato, K., Kumasaka, T., Yamamoto, M., Ishii, S., Ogata, K., 2001. Structural analyses of DNA recognition by the AML1/Runx-1 Runt domain and its allosteric control by CBFbeta. Cell 104, 755–767.

Takeda, S., Bonnamy, J.P., Owen, M.J., Ducy, P., Karsenty, G., 2001. Continuous expression of Cbfa1 in nonhypertrophic chondrocytes uncovers its ability to induce hypertrophic chondrocyte differentiation and partially rescues Cbfa1-deficient mice. Genes Dev. 15, 467–481.

Thirunavukkarasu, K., Mahajan, M., McLarren, K.W., Stifani, S., Karsenty, G., 1998. Two domains unique to osteoblast-specific transcription factor Osf2/Cbfa1 contribute to its transactivation function and its inability to heterodimerize with Cbfbeta. Mol. Cell. Biol. 18, 4197–4208.

Ueta, C., Iwamoto, M., Kanatani, N., Yoshida, C., Liu, Y., Enomoto-Iwamoto, M., Ohmori, T., Enomoto, H., Nakata, K., Takada, K., Kurisu, K., Komori, T., 2001. Skeletal malformations caused by overexpression of Cbfa1 or its dominant negative form in chondrocytes. J. Cell. Biol. 153, 87–100.

Vidal, O., Lindberg, M.K., Hollberg, K., Baylink, D.J., Andersson, G., Lubahn, D.B., Mohan, S., Gustafsson, J.A., Ohlsson, C., 2000. Estro-

gen receptor specificity in the regulation of skeletal growth and maturation in male mice. Proc. Natl. Acad. Sci. U. S. A. 97, 5474–5479.

Vortkamp, A., Lee, K., Lanske, B., Segre, G.V., Kronenberg, H.M., Tabin, C.J., 1996. Regulation of rate of cartilage differentiation by Indian hedgehog and PTH-related protein. Science 273, 613–622.

Wang, Q., Stacy, T., Miller, J.D., Lewis, A.F., Gu, T.L., Huang, X., Bushweller, J.H., Bories, J.C., Alt, F.W., Ryan, G., Liu, P.P., Wynshaw-Boris, A., Binder, M., Marin-Padilla, M., Sharpe, A.H., Speck, N.A., 1996. The CBFbeta subunit is essential for CBFalpha2 (AML1) function in vivo. Cell 87, 697–708.

Wang, W.F., Wang, Y.G., Reginato, A.M., Plotkina, S., Gridley, T., Olsen, B.R., 2002. Growth defect in Grg5 null mice is associated with reduced Ihh signaling in growth plates. Dev. Dyn. 224, 79–89.

Weise, M., De-Levi, S., Barnes, K.M., Gafni, R.I., Abad, V., Baron, J., 2001. Effects of estrogen on growth plate senescence and epiphyseal fusion. Proc. Natl. Acad. Sci. U. S. A. 98, 6871–6876.

Westendorf, J.J., Zaidi, S.K., Cascino, J.E., Kahler, R., van Wijnen, A.J., Lian, J.B., Yoshida, M., Stein, G.S., Li, X., 2002. Runx2 (Cbfa1, AML-3) interacts with histone deacetylase 6 and represses the p21(CIP1/WAF1) promoter. Mol. Cell. Biol. 22, 7982–7992.

Yang, Y., Topol, L., Lee, H., Wu, J., 2003. Wnt5a and Wnt5b exhibit distinct activities in coordinating chondrocyte proliferation and differentiation. Development 130, 1003–1015.

Yao, J., Liu, Y., Husain, J., Lo, R., Palaparti, A., Henderson, J., Stifani, S., 1998. Combinatorial expression patterns of individual TLE proteins during cell determination and differentiation suggest non-redundant functions for mammalian homologs of *Drosophila* Groucho. Dev. Growth Differ. 40, 133–146.

Yoshida, C.A., Furuichi, T., Fujita, T., Fukuyama, R., Kanatani, N., Kobayashi, S., Satake, M., Takada, K., Komori, T., 2002. Core-binding factor beta interacts with Runx2 and is required for skeletal development. Nat. Genet. 32, 633–638.